International Journal of Power Electronics and Drive Systems (IJPEDS)
Vol. 12, No. 3, September 2021, pp. 1853~1861
ISSN: 2088-8694, DOI: 10.11591/ijpeds.v12.i3.pp1853-1861

H7 three phase transformerless inverter for photovoltaic grid-tied system with maximum power point operation

Essam Hendawi[1], Sherif Zaid[2]
[1]Electrical Engineering Department, College of Engineering, Taif University, Taif, Kingdom of Saudi Arabia
[2]Department of Electrical Power, Faculty of Engineering, Cairo University, Cairo, Egypt

Article Info

Article history:

Received Apr 1, 2021
Revised Jul 12, 2021
Accepted Jul 23, 2021

Keywords:

Grid-tied system
Leakage current minimization
Maximum power point
Renewable energy sources
Transformerless inverter

ABSTRACT

One of the most important and common parts of the modern power systems is the grid-connected photovoltaic (PV) systems. Recently, these systems have gotten a big revolution due to the introduction of the transformerless inverters. It has the merits of small size, low cost, and high efficiency. However, transformerless inverters has a general safety problem related to the earth leakage current. Various researches were directed toward evolving their performance and diminishing the leakage current to the standard limits. This article proposes an application of the H7 controller to a PV powered grid-tied three phase transformerless inverter. The transformerless inverter is linked with the grid through a boost converter. The boost converter inductance is rearranged and divided to reduce the earth leakage current of the system. simulations are carried out for the proposed H7 PV grid-tied system and for a system that uses the conventional three phase inverter. The simulation results show that the H7 inverter provides lower leakage current, higher efficiency, and lower total harmonic distortion (THD) compared to the conventional three phase inverter.

Corresponding Author:

Essam Hendawi
Departement of Electrical Engineering
Taif University
Taif, Kingdom of Saudi Arabia
Email: essam@tu.edu.sa

1. INTRODUCTION

Solar photovoltaic (PV) energy sources have gained great importance in recent years. It is one of the most promising renewable energy sources that can meet the increasing demands of electrical energy in the future. PV sources can also overcome the problems of environmental pollution [1]. PV systems could deliver energy to electric utility grid or standalone loads. Grid tied PV systems have several advantages over standalone ones where optimum utilization of PV panels can be achieved without any storage requirement [2].

In PV grid-connected systems, a transformer is employed to achieve several targets; (1) raising the PV panels voltage to suitable levels that meet requirements of connection to the grid, (2) preventing the injection of DC currents into the grid and therefore it improves the grid power quality and (3) providing galvanic isolation between the PV panels and the grid thus achieving personal safety where it prevents the leakage current which can flow in the parasitic capacitance between the frame of PV panels and ground. On the other hand, the transformer results in increase in size, weight and cost of PV systems and also the efficiency is decreased [3]-[5]. Transformerless inverters overcome the aforementioned disadvantages of transformers. Several single phase and three phase topologies of transformerless inverters are presented in the

literature [6]-[13]. Single phase transformerless inverters are usually small-scale up to 5–6kW. Large DC link capacitors are required to overcome the pulsation in the output power. These capacitors decrease the reliability and lifetime of the system [14]. On the other hand, in transformerless inverters systems, the ac power on the output is constant, which means that large capacitors are not needed, resulting to smaller cost, and a higher reliability and longer lifetime of the whole system. Three phase transformerless inverter systems rather than single phase ones are usually employed in high power applications. Most transformerless are oriented to control the changes in common mode voltage and consequently reduce the leakage current to safe limits. The absence of maximizing the power drawn from the PV panels with reducing the ground leakage current is clearly observed [15]-[20]. The problem this paper is addressing is the leakage current minimization in three phase grid tied PV systems with achievement of maximum power operation of PV panels. H7 three phase transformerless inverter operated at SVPWM is utilized to overcome the problem of leakage current. DC-DC boost converter that is controlled by a maximum power point tracker MPPT is introduced to maximize the delivered power from PV arrays. Input voltage of the inverter is maintained constant by a voltage controller. Three phase LC filter is used to cancel high frequency harmonics. The paper is organized as follows: Section 2 introduces the techniques of ground leakage current minimization. H7 operation and its modulation techniques are presented in section 3. The overall system and controllers are proposed in section 4. Section 5 provides the simulation results and discussion of the proposed system. Section 6 provides the net conclusions of the paper.

2. LEAKAGE CURRENT MINIMIZATION TECHNIQUES

The ground leakage current finds its path through the parasitic capacitance (C_{PV}) between the frame of PV panels and ground. The common mode voltage of the three-phase transformerless inverter is presented to study its influence on the leakage ground current. The German standard, VDE0126-1-1, shows the requirements for limits regarding ground leakage currents [21]. With respect to three phase transformerless inverters, the presented techniques to minimize the leakage current can be divided into two main categories. The first is based on modulation techniques and the second is based on the configurations of the topologies. The following sections introduce brief descriptions about the two categories.

2.1. Leakage current minimization based on modulation techniques

Reduced common mode voltage pulse width modulation (RCMV-PWM) techniques have been presented to reduce the common mode voltage and consequently reduce the ground leakage current. The most popular ones are near-state PWM (NSPWM) [22], remote-state PWM (RSPWM) [23] and active zero-state PWM (AZPWM) [24]. Unlike the conventional sinusoidal PWM (SPWM) and space vector PWM (SVPWM), the RCMV-PWM techniques do not apply the zero vectors V_0 (000) or V_7 (111) to the inverter operation. Instead, the RCMV-PWM techniques apply only the active vectors V_1 through V_6 to the inverter. The selection of active vectors over each switching period depends on the location of the voltage command in the dq plane and the type of operation (type A or type B). Figure 1 (a) and Figure 1 (b) give the active vectors and the six sectors (A_1 to A_6 for type A operation) and (B_1 to B_6 for type B operation). AZPWM and RSPWM are applied in type 'A' while NSPWM is applied in type 'B'. Table 1 summarizes the patterns of vectors during each sector when applying SVPWM and the RCMV-PWM techniques.

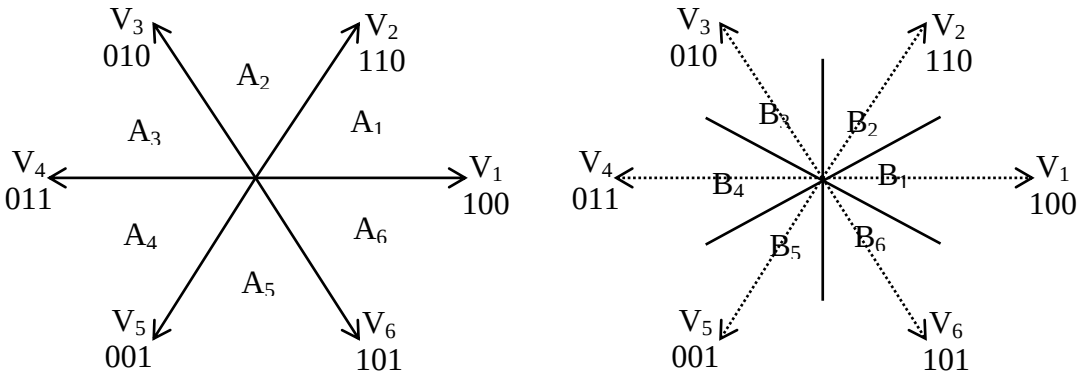

Figure 1. Voltage vectors and sectors for the two types A and B

Table 1. Patterns of vectors during each sector when applying svpwm and the RCMV-PWM

Sector	SVPWM	AZPWM	RSPWM	Sector	NSPWM
A_1	7210127	6123216	31513 or 42624 in all sectors	B_1	21612
A_2	7230327	4321234		B_2	32123
A_3	7430347	2345432		B_3	43234
A_4	7450547	6543456		B_4	54345
A_5	7650567	4561654		B_5	65456
A_6	7610167	2165612		B_6	16561

Although the RCMV-PWM techniques reduce the ground leakage current to very small values, other system performance such as voltage linearity, output current ripples, inverter losses and total harmonic distortion are degraded. In addition, there are limitations on modulation index when applying either NSPWM or RSPWM [25]. When applying RSPWM, very high input voltage is required to inject the real power to the grid resulting in increase in losses and THD.

2.2. Leakage current minimization based on inverter configuration

Another approach to reduce the leakage current is based on inverter configuration. Different topologies are presented [10], [11]. Three phase full bridge VSI with split capacitor (3FB-SC) and three phase neutral point clamped VSI (3xNPC) reduce the leakage to very low values while conventional three phase full bridge VSI (3FB) has a high leakage current and then strongly requires a galvanic isolation [11]. 3FB inverter has a high leakage current when connected to grid and therefore requires a galvanic isolation. On the other hand, 3FB-SC and 3xNPC greatly reduce the leakage current below the limited vales. The main disadvantage is the influence of the inductance in the neutral line which can result in leakage current higher than the allowed levels. In addition, large number of power switches and diode is required in case of 3xNPC inverter which increase the losses, system complexity and cost. Recent topologies such as three phase VSI with 4-legs, H8 converter topology and flying capacitor transformer-less inverter are presented [26]-[28] and successfully reduce the leakage current. However, the three topologies have many semiconductor elements which also increase the losses, system complexity and cost.

3. H7 OPERATION AND ITS MODULATION TECHNIQUE

H7 three phase transformerless inverter represents a very suitable solution to reduce the ground leakage current while adding only one switch to the conventional three phase bridge inverter as shown in Figure 2. H7 transformerless inverter is considered as extension version of well-known H5 single phase transformerless inverter. This section presents the proposed system configuration, system analysis and principle of operation of H7 three phase transformer-less inverter.

The basic idea of H7 inverter is to disconnect the PV panels from the grid during freewheeling periods and as a result there will be no path for leakage current. The seventh switch S7 conducts during active modes (vectors V1 to V6) and it is forced to 'off' state during freewheeling periods (vectors V_0 and V_7). A simplified equivalent circuit of H7 inverter with the grid is presented in Figure 3 including LC filter, parasitic capacitance and ground inductance L_g.

Referring to Figure 2 and during the active mode V_2 (110), the switches S_1, S_3 and S_2 conduct together. The inverter phase voltages and common mode voltage becomes:

$$V_{AN} = V_{BN} = \frac{V_{dc}}{3} \quad (1)$$

$$V_{CN} = \frac{-2V_{dc}}{3} \quad (2)$$

The inverter terminal voltages with respect to the negative terminal of the DC link voltage are:

$$V_{A-} = V_{B-} = V_{dc} \quad (3)$$

$$V_{C-} = zero \quad (4)$$

The common mode voltage in this case is:

$$V_{CMV} = \frac{(V_{A-} + V_{B-} + V_{C-})}{3} = \frac{2V_{dc}}{3} \quad (5)$$

The same calculations can be carried out for the other five active vectors. The results are summarized in Table 2. When applying the zero vector V_7, freewheeling operation occurs. The current paths through one of the upper switches and two antiparallel diodes of the other two switches depending on the voltage levels of the grid. During this freewheeling period:

$$V_{A-} = V_{B-} = V_{C-} = V_{dc} \quad (6)$$

and

$$V_{CMV} = V_{dc} \quad (7)$$

When applying the zero vector V_0, freewheeling operation occurs. The current passes through two switches of the lower switches and one antiparallel diode of the third switch depending on the voltage levels of the grid. During this freewheeling period:

$$V_{A-} = V_{B-} = V_{C-} = zero \quad (8)$$

and

$$V_{CMV} = zero \quad (9)$$

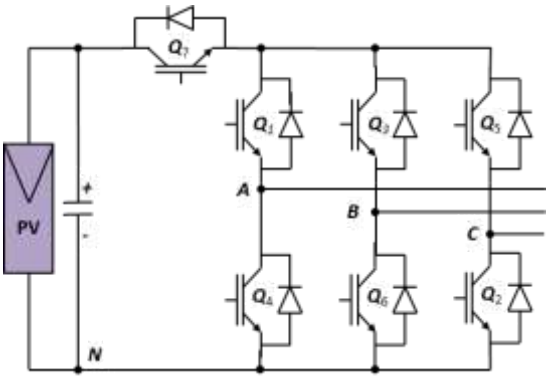

Figure 2. H7 transformerless inverter

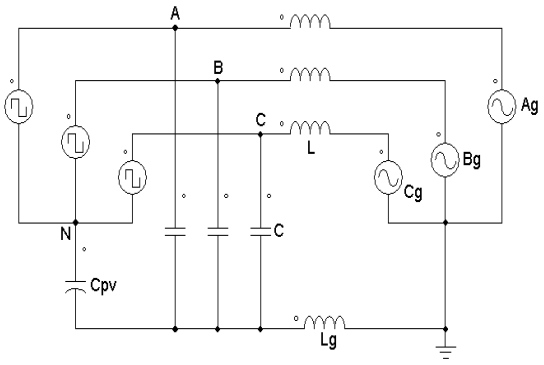

Figure 3. Simplified equivalent circuit of H7 inverter with the grid

4. OVERALL SYSTEM AND CONTROLLERS

The proposed system is presented in Figure 4. The main part, H7 transformerless inverter, is the previously mentioned. The system includes DC-DC boost converter, LC filter, maximum power point tracker and controllers. The following subsections describe each of those controllers. Method of controlling the extracted power from PV panels, boost converter and H7 transformer-less inverter switches are proposed in this section.

4.1. DC-DC boost converter and controller

The well-known DC-DC boost converter is utilized to raise the voltage of PV panels to meet the grid requirements. The switch of the boost converter is controlled by a maximum power point tracker to extract the maximum power from the PV panels. The inductor of the boost converter is connected in series with the PV panels the current of which is controlled through a hysteresis current controller in such a way that the PV panels' current always follow the current associated to the maximum power point at any level of sun irradiance level. A look-up table that relates the maximum power point with the corresponding current is formed at different irradiance level and is then employed to set the required reference current for the hysteresis current controller.

4.2. Boost converter voltage controller

The boost converter output voltage (input voltage to the inverter) must be maintained constant (650V) in three phase system. This is achieved by a voltage controller which is presented in Figure 5 [29]. The controller combines the simplicity of classical controller and behaves like intelligent controller at the

same time. The controller compares the reference voltage (650 V) with two quantities; the actual boost voltage and its derivative multiplied by gain 1. The error is applied to gain 2 then the integrator to give the reference grid current $I_{G\text{-}ref}$.

4.3. H7 inverter control signals

Actual grid current I_g, actual grid voltage V_g and reference grid current $I_{G\text{-}ref}$ are employed to generate the control signals of the seven switches. Phase locked loop (PLL) is applied to V_g and PI controller is used to generate the modulating voltage which is utilized to generate the high frequency control signal and its complement for each leg of the inverter. Zero voltage vectors V_0 and V_7 are applied during freewheeling periods as previously discussed in section 3. The phase locked loop (PLL) achieves synchronization between the PV array and the grid.

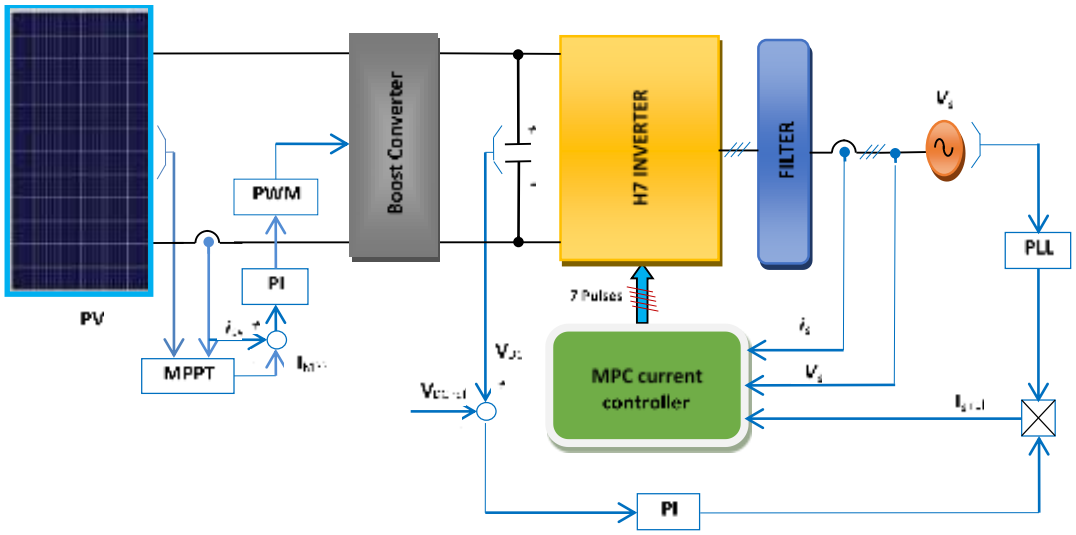

Figure 4. The proposed overall system

Table 2. Inverter phase voltages and common mode voltage when applying active vectors

	V_1	V_2	V_3	V_4	V_5	V_6
V_{AN}	$2V_{DC}/3$	$V_{DC}/3$	$-V_{DC}/3$	$-2V_{DC}/3$	$-V_{DC}/3$	$V_{DC}/3$
V_{BN}	$-V_{DC}/3$	$V_{DC}/3$	$2V_{DC}/3$	$V_{DC}/3$	$-V_{DC}/3$	$-2V_{DC}/3$
V_{CN}	$-V_{DC}/3$	$-2V_{DC}/3$	$-V_{DC}/3$	$V_{DC}/3$	$2V_{DC}/3$	$V_{DC}/3$
V_{A-}	V_{DC}	V_{DC}	0	0	0	V_{DC}
V_{B-}	0	V_{DC}	V_{DC}	V_{DC}	0	0
V_{C-}	0	0	0	V_{DC}	V_{DC}	V_{DC}
V_{CMV}	$V_{DC}/3$	$2V_{DC}/3$	$V_{DC}/3$	$2V_{DC}/3$	$V_{DC}/3$	$2V_{DC}/3$

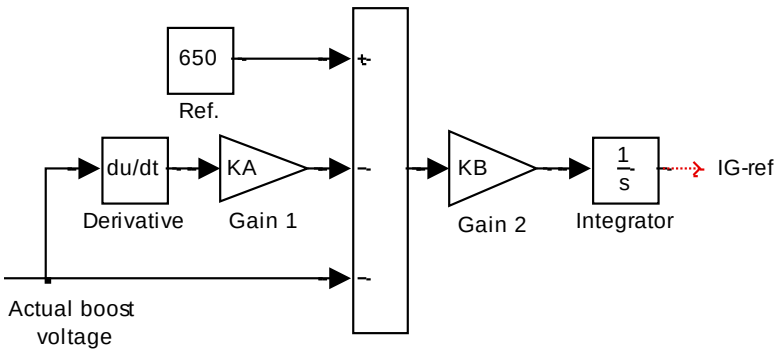

Figure 5. Boost converter voltage controller

5. SIMULATION RESULTS

The performance evaluation obtained through system operation and simulation results is presented in this section using MATLAB/Simulink package. The system parameters are given in Table 3. Figure 6 shows the the results of the proposed H7 transformerless inverter versus the results with the conventional 3-φ six switch inverters. Both of the topologies are controlled by PI current controller, and they operate with sinusoidal pulse width modulation SPWM. The new configuration of the boost converter is applied for each topology. The three phase grid currents are sinusoidal and in phase with the grid voltage, with the two controllers, thus (unity power factor) is achieved. The grid current THD with the H7 controller is 2.43% and that with the conventional topology is 2.45%. As the controller action in each case is different, the line voltages of inverter output have different waveforms. On the other hand, and as the same MPPT is employed for each case, the PV currents are the same for the two controllers. Based on leakage current, it can be noticed that the H7 topology case has a much smaller current than the other topology.

Figure 7 presents the variations of the RMS value of the earth leakage current as the sun irradiance level varies. In the case of the H7 topology, the leakage current value is smaller than the value of the conventional 3-φ inverter. However, at 10% insolation, vice versa occurs. The leakage current value does not exceed the standard of 300 mA for the two cases. Figure 8 gives the variations of grid current frequency spectrum of the at sun irradiance level of 100%.

The figure shows that in the H7 case, lower order harmonics are slightly higher than lower order harmonics in case of the conventional 3-φ inverter. Generally, the THD value of the two cases are very close. Figure 9 gives the response of the inverter output power and the maximum PV extracted power in the case of H7 Figure 9 (a) and the conventional 3-φ inverter Figure 9 (b). The inverter output power tracks the MPP power in the two cases with an expected steady state error which represents system losses. In the H7 controller case, the losses are smaller than that in the conventional 3-φ inverter case. This difference is due to a small THD which produces harmonic losses. With increasing power levels, losses increase. This is considered as a normal issue because current values increase with the increase in power levels. Figure 10 presents the variation of system efficiency as sun irradiance level changes for the H7 controller and conventional 3-φ inverter. Under all irradiance levels, the efficiency in case of H7 inverter is higher than that for the conventional 3-φ inverter.

Table 3. System parameters

Parameter	Value
PV short circuit current	24.53 A
PV open circuit voltage	633 V
C_{earth}	200 nF
DC link voltage V_{DC}	650 V
L_f	3 mH
C_f	2 µF
Grid frequency	50 Hz
Grid voltage	230 V
PWM carrier frequency	9 KHz
DC link capacitor	1000 µF

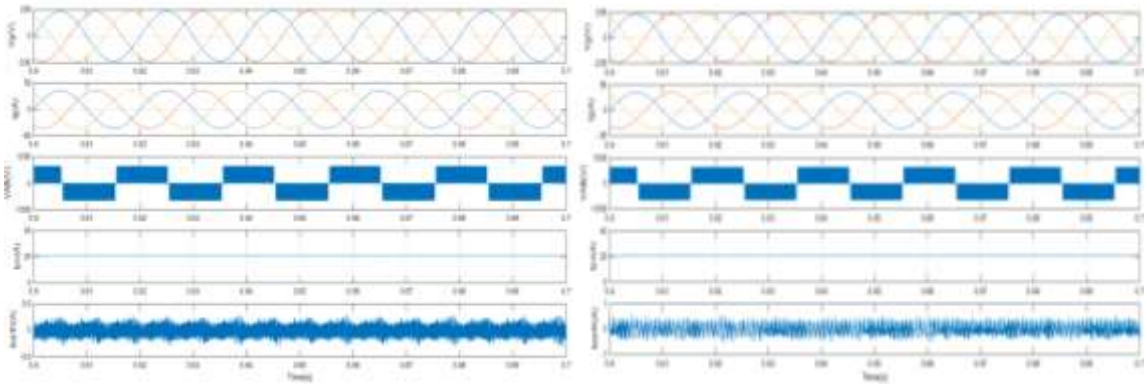

(a) (b)

Figure 6. Simulation results of (a) the proposed H7 transformerless inverter grid voltage, grid current, PV panels' current, and ground leakage current and (b) the conventional 3-φ inverter

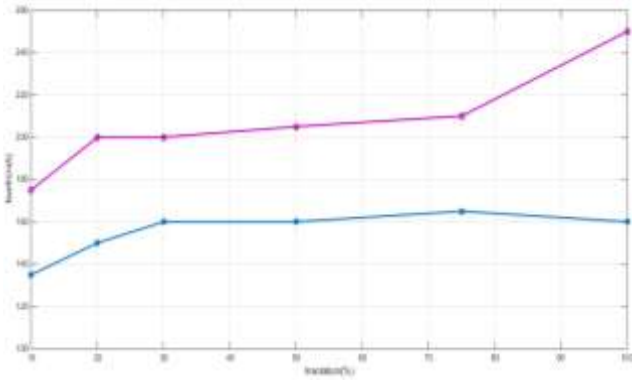

Figure 7. The variations of the ground leakage current with the sun irradiance level for the H7 inverter and the conventional 3-φ inverter

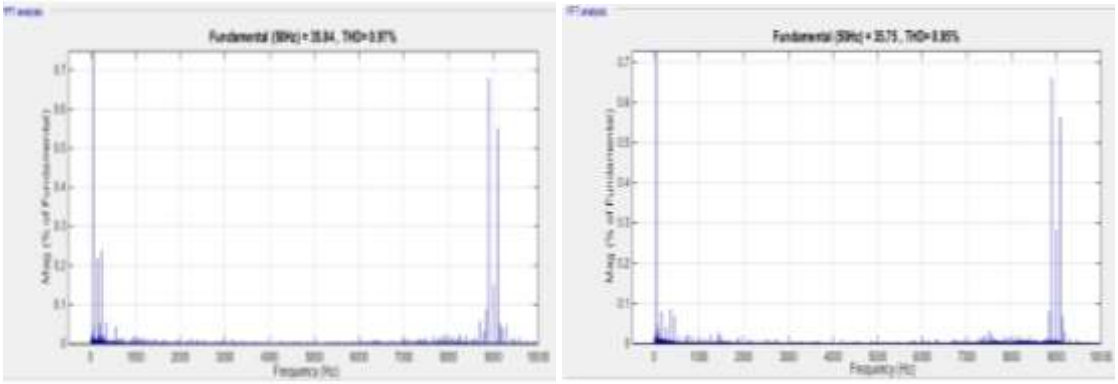

(a) (b)

Figure 8. The grid current frequency spectrum for the (a) H7 inverter and (b) the conventional 3-φ inverter (@100% insolation)

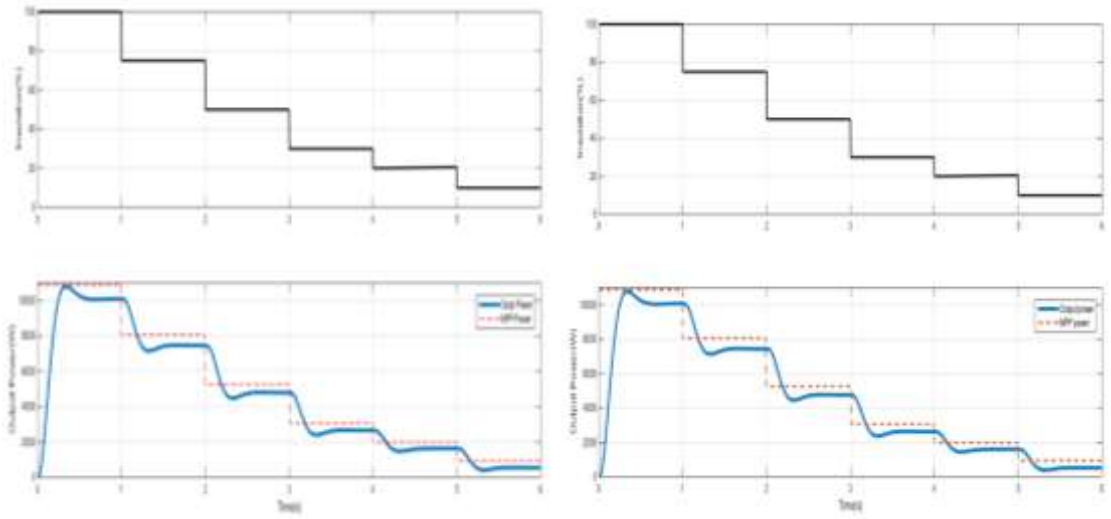

(a) (b)

Figure 9. The MPP power, output power with variations in sun irradiance for (a) H7 topology and (b) conventional 3-φ inverter

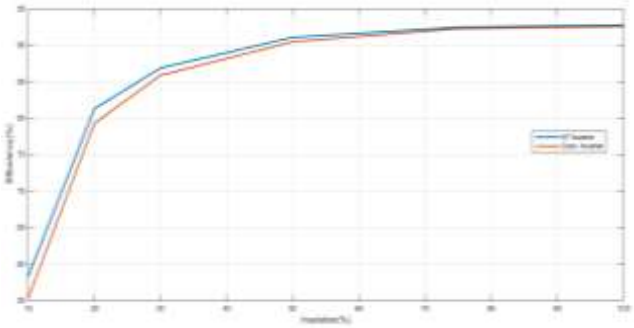

Figure 10. The system efficiency variations with variations in sun irradiance level for the H7 inverter and the conventional 3-φ inverter

6. CONCLUSION

This article proposed an application of the H7 controller to a PV powered grid-tied 3-φ transformerless inverter. The presented transformerless inverter is connected to the grid through a boost converter. The boost converter inductance is rearranged and divided to reduce the earth leakage current of the system. MATLAB simulations for the proposed H7 system and for a system that uses the conventional 3-φ inverter were carried out. Simulation results; i) The H7 inverter has better performance over conventional 3-φ inverter for all factors of comparison, ii) the three phase grid currents, when applying the two controllers, are sinusoidal and in phase with the utility grid voltage thus unity power factor is achieved, and iii) the THD of the grid current with the H7 inverter is 2.43% and that with conventional 3-φ inverter is 2.45%. The leakage current with the H7 inverter case is less than the value with the conventional 3-φ inverter. The efficiency of the system that uses H7 inverter is improved compared to a system that uses a conventional 3-φ inverter.

REFERENCES

[1] F. Blaabjerg, R. Teodorescu, M. Liserre and A. V. Timbus, "Overview of control and grid synchronization for distributed power generation systems," in *IEEE Transactions on Industrial Electronics*, vol. 53, no. 5, pp. 1398-1409, Oct. 2006, doi: 10.1109/TIE.2006.881997.

[2] S. B. Kjaer, J. K. Pedersen and F. Blaabjerg, "A review of single-phase grid-connected inverters for photovoltaic modules," in *IEEE Transactions on Industry Applications*, vol. 41, no. 5, pp. 1292-1306, Sept.-Oct. 2005, doi: 10.1109/TIA.2005.853371.

[3] D. Meneses, F. Blaabjerg, O. Garc´ıa and J. A. Cobos, "Review and comparison of step-up transformerless topologies for photovoltaic AC-module application", *IEEE Transactions on Power Electronics*, vol. 28, no. 6, June 2013

[4] G. Rizzoli, M. Mengoni, L. Zarri, A. Tani, G. Serra, and D. Casadei, "Comparison of single-phase H4, H5, H6 inverters for transformerless photovoltaic applications," *IECON 2016 - 42nd Annual Conference of the IEEE Industrial Electronics Society*, 2016, pp. 3038-3045, doi: 10.1109/IECON.2016.7792984.

[5] L. A. Kumar, V. Indragandhi, and N. S. Kumar, "Design and implementation of single-phase inverter without transformer for PV applications," *IET Renewable Power Generation*, vol. 12, no. 5, pp. 547-554, Mar 2018, doi: 10.1049/iet-rpg.2017.0257.

[6] E. Hendawi, "A high performance grid connected PV system based on HERIC transformerless inverter," *Indonesian Journal of Electrical Engineering and Computer Science*, vol. 20, no. 2, pp. 602-612, Nov. 2020, doi: 10.11591/ijeecs.v20.i2.pp602-612.

[7] M. N. H. Khan, M. Forouzesh, Y. P. Siwakoti, L. Li, T. Kerekes, and F. Blaabjerg, "A Classification of single-phase transformerless inverter topologies for photovoltaic applications," *2018 IEEE Region Ten Symposium (Tensymp)*, 2018, pp. 174-179, doi: 10.1109/TENCONSpring.2018.8692013.

[8] Suroso, and H. Siswantoro, "A performance comparison of transformer-less grid tied PV system using diode clamped and neutral point shorted inverters," *International Journal of Power Electronics and Drive System (IJPEDS)*, vol. 11, no. 2, pp. 702-710, June 2020, doi: 10.11591/ijpeds.v11.i2.pp702-710.

[9] E. Hendawi and S. Zaid, "Grid connected PV system with maximum power point achievement based on H5 transformerless inverter," *Journal of Electrical Engineering*, Vol. 17, Issue 4, 2017.

[10] T. Kerekes, R. Teodorescu, M. Liserre, C. Klumpner, and M. Sumner, "Evaluation of three-phase transformerless photovoltaic inverter topologies," in *IEEE Transactions on Power Electronics*, vol. 24, no. 9, pp. 2202-2211, Sept. 2009, doi: 10.1109/TPEL.2009.2020800.

[11] I. C. Rath, and A. Shukla, "Review of Three Phase Transformer-less PV Converters," *2019 IEEE International Conference on Sustainable Energy Technologies and Systems (ICSETS)*, 2019, pp. 063-068, doi: 10.1109/ICSETS.2019.8745120.
[12] H. Albalawi, and S. A. Zaid, "Performance improvement of a grid-tied neutral-point-clamped 3-ϕ transformerless inverter using model predictive control," *Processes*, vol. 7, no. 11, 2019, Nov. 2019, doi: 10.3390/pr7110856.
[13] N. S. Jayalakshmi, A. Kumar, and A. Kumar, "Analysis and design of single phase high efficiency transformer less PV inverter topology," *International Journal of Power Electronics and Drive System (IJPEDS)*, Vol. 9, No. 2, pp. 730-737, June 2018, doi: 10.11591/ijpeds.v9.i2.pp730-737.
[14] G. Petrone, G. Spagnuolo, R. Teodorescu, M. Veerachary, and M. Vitelli, "Reliability issues in photovoltaic power processing systems," in *IEEE Transactions on Industrial Electronics*, vol. 55, no. 7, pp. 2569-2580, July 2008, doi: 10.1109/TIE.2008.924016.
[15] M. C. Cavalcanti, K. C. de Oliveira, A. M. de Farias, F. A. S. Neves, G. M. S. Azevedo, and F. C. Camboim, "Modulation techniques to eliminate leakage currents in transformerless three-phase photovoltaic systems," in *IEEE Transactions on Industrial Electronics*, vol. 57, no. 4, pp. 1360-1368, April 2010, doi: 10.1109/TIE.2009.2029511.
[16] A. K. Gupta, H. Agrawal, and V. Agarwal, "A novel three-phase transformerless H-8 topology with reduced leakage current for grid-tied solar PV applications," in *IEEE Transactions on Industry Applications*, vol. 55, no. 2, pp. 1765-1774, March-April 2019, doi: 10.1109/TIA.2018.2883372.
[17] F. Bradaschia, M. C. Cavalcanti, P. E. P. Ferraz, F. A. S. Neves, E. C. dos Santos, and J. H. G. M. da Silva, "Modulation for three-phase transformerless z-source inverter to reduce leakage currents in photovoltaic systems," in *IEEE Transactions on Industrial Electronics*, vol. 58, no. 12, pp. 5385-5395, Dec. 2011, doi: 10.1109/TIE.2011.2116762.
[18] X. Guo, "Three-phase CH7 inverter with a new space vector modulation to reduce leakage current for transformerless photovoltaic systems," in *IEEE Journal of Emerging and Selected Topics in Power Electronics*, vol. 5, no. 2, pp. 708-712, June 2017, doi: 10.1109/JESTPE.2017.2662015.
[19] X. Wang, J. Zou, L Ma., J. Zhao, C. Xie, K. Li, L. Meng, and J.M. Guerrero, "Model predictive control methods of leakage current elimination for a three-level T-type transformerless PV inverter," *IET Power Electronics*, vol. 11, pp. 1492-1498, 2018, doi: 10.1049/iet-pel.2017.0762
[20] R. Vargas, P. Cortes, U. Ammann, J. Rodriguez, and J. Pontt, "Predictive control of a three-phase neutral-point-clamped inverter," in *IEEE Transactions on Industrial Electronics*, vol. 54, no. 5, pp. 2697-2705, Oct. 2007, doi: 10.1109/TIE.2007.899854.
[21] VDE 0126-1-1-2006, "Automatic disconnection device between a generator and the public low-voltage grid," DIN_VDE Normo, 2008.
[22] E. Un, and A. M. Hava, "A near-state PWM method with reduced switching losses and reduced common-mode voltage for three-phase voltage source inverters," in *IEEE Transactions on Industry Applications*, vol. 45, no. 2, pp. 782-793, March-april 2009, doi: 10.1109/TIA.2009.2013580.
[23] M. Cacciato, A. Consoli, G. Scarcella, and A. Testa, "Reduction of common-mode currents in PWM inverter motor drives," in *IEEE Transactions on Industry Applications*, vol. 35, no. 2, pp. 469-476, March-April 1999, doi: 10.1109/28.753643.
[24] G. Oriti, A. L. Julian, and T. A. Lipo, "A new space vector modulation strategy for common mode reduction," in *Proc. IEEE PESC*, Jun. 1997, pp. 1541–1546.
[25] T. K. S. Freddy, N. A. Rahim, W. Hew, and H. S. Che, "Modulation techniques to reduce leakage current in three-phase transformerless H7 photovoltaic inverter," in *IEEE Transactions on Industrial Electronics*, vol. 62, no. 1, pp. 322-331, Jan. 2015, doi: 10.1109/TIE.2014.2327585.
[26] F. Hasanzad, H. Rastegar, and M. Pichan, "Performance evaluation of space vector modulation techniques for reducing leakage current of a three-phase four-leg PV inverter," *2017 Iranian Conference on Electrical Engineering (ICEE)*, 2017, pp. 1026-1031, doi: 10.1109/IranianCEE.2017.7985190.
[27] C. T. Morris, D. Han, and B. Sarlioglu, "Reduction of common mode voltage and conducted EMI through three-phase inverter topology," in *IEEE Transactions on Power Electronics*, vol. 32, no. 3, pp. 1720-1724, March 2017, doi: 10.1109/TPEL.2016.2608388.
[28] X. Guo *et al*., "Leakage current suppression of three-phase flying capacitor PV inverter with new carrier modulation and logic function," in *IEEE Transactions on Power Electronics*, vol. 33, no. 3, pp. 2127-2135, March 2018, doi: 10.1109/TPEL.2017.2692753.
[29] M. M. Salem, "Classical controller with intelligent properties for speed of vector controlled induction motor," in *Journal of Power Electronics*, vol. 8, no. 3, pp. 210- 216, July 2008.